

# Synthesis and Characterization of Fe<sub>3</sub>O<sub>4</sub> Nanoparticles Modified with Polyethylene Glycol as Antibacterial Material

Poedji Loekitowati Hariani<sup>1\*</sup>, Desnelli<sup>1</sup>, Fatma<sup>1</sup>, Rizki Indah Putri<sup>1</sup>, and Salni<sup>2</sup>

<sup>1</sup>Department of Chemistry, Faculty of Mathematics and Natural Sciences, Sriwijaya University

<sup>2</sup>Department of Biology, Faculty of Mathematics and Natural Sciences, Sriwijaya University  
Jalan Palembang-Prabumulih Km 32 Inderalaya OI, Indonesia

\*Corresponding author: puji\_lokitowati@mipa.unsri.ac.id

Received 24 November 2017; Revised 1 March 2018; Accepted 1 March 2018

## ABSTRACT

The iron oxide (Fe<sub>3</sub>O<sub>4</sub>) nanoparticles modified with polyethylene glycol (PEG) was synthesized by co-precipitation methods using ferric and ferrous ions as the precursors. Further, the antibacterial activity was performed against gram-positive and gram-negative bacteria. The Fe<sub>3</sub>O<sub>4</sub>-PEG was characterized using X-Ray Diffraction (XRD), Fourier Transform Infra Red (FTIR), Scanning Electron Microscopy (SEM) with energy dispersive X-Ray analysis (EDAX) and Vibrating Sample Magnetometer (VSM). The particle size of Fe<sub>3</sub>O<sub>4</sub>-PEG calculated using XRD is 46.2 nm. The study confirmed that Fe<sub>3</sub>O<sub>4</sub>-PEG is superparamagnetic and has a saturation magnetization of 56.43 emu/g. The prepared Fe<sub>3</sub>O<sub>4</sub>-PEG gives the effect of both gram-positive and gram-negative pathogenic bacterial strains hence this material has potential utilization in the field of pharmaceutical and biomedical in the future.

Keyword: Fe<sub>3</sub>O<sub>4</sub>, nanoparticle, PEG, antibacterial activity

## INTRODUCTION

In recent years, spinel ferrite nanoparticles have been the subject of developed research. The dimension of nanoparticle is between bulk materials and atoms or molecules. The spinel ferrite has a structural formula MFe<sub>2</sub>O<sub>4</sub>, where M is a divalent metal with a cubic spinel crystal structure. In addition, the spinel ferrite has magnetic properties. Magnetic nanoparticles can be used in various applications such as adsorbent [1,2], magnetic storage, ferrofluids, biomedical applications [3,4] and gas sensor [5].

Various methods can be used to prepare magnetic nanoparticles such as co-precipitation [6,7], hydrothermal [8], microemulsion [9], electrochemical route [10,11] and sol-gel [12]. One of the magnetic nanoparticles is Fe<sub>3</sub>O<sub>4</sub> (magnetite). The materials exhibit superparamagnetic behavior, low toxicity, biocompatibility, easier surface modification [13,14].

Another study reported that Fe<sub>3</sub>O<sub>4</sub> magnetic nanoparticles have antibacterial activity properties. Fe<sub>3</sub>O<sub>4</sub> nanoparticles showed strong antibacterial activity, the antibacterial activity caused by the presence of reactive oxygen species (ROS) [4]. The Fe<sub>3</sub>O<sub>4</sub> nanoparticle has the greatest antibacterial effect to pathogenic bacteria of *Pseudomonas aeruginosa* than *Escherichia coli* and *Staphylococcus aureus* [15]. In addition, the Fe<sub>3</sub>O<sub>4</sub> nanoparticle has a zone of inhibition consideration to Ag nanoparticle for topical use [14].

The journal homepage [www.jpacr.ub.ac.id](http://www.jpacr.ub.ac.id)  
p-ISSN : 2302 – 4690 | e-ISSN : 2541 – 0733

Materials in the form of small particle sizes are easy to agglomerate and made it larger particle size, reducing surface area and magnetic properties. Agglomeration can be prevented by coating nanoparticles with organic polymeric materials. The coating process also prevents nanoparticles from oxidation processes, reduces toxicity and increases chemical stability [16,17]. Some research on coating nanoparticles with organic materials such as CoFe<sub>2</sub>O<sub>4</sub>-alginate [18], Fe<sub>3</sub>O<sub>4</sub>-polypropylene [8], CoFe<sub>2</sub>O<sub>4</sub>-chitosan [19], CoFe<sub>2</sub>O<sub>4</sub>-polyvinyl alcohol, gelatin [16].

In this study, we used co-precipitation method for preparing Fe<sub>3</sub>O<sub>4</sub> and coating with polyethylene glycol (PEG)-4000. PEG is long polymer chains with several advantages for coating Fe<sub>3</sub>O<sub>4</sub> of non-toxic to a large extent, non-immunogenic, non-antigenic, and protein-resistant polymer [16,20]. In addition, the incorporation of inorganic and organic particles has combination of the properties of inorganic particles such as thermal, mechanical, magnetic, and the properties of organic particles that is flexibility. Furthermore, the Fe<sub>3</sub>O<sub>4</sub>-PEG were evaluated for antibacterial activities. The bacteria used are gram-positive (*Staphylococcus aureus*) and gram-negative (*Escherichia coli*).

## EXPERIMENT

### Chemicals and instrumentation

The chemical reagents used in this study were FeCl<sub>3</sub>.6H<sub>2</sub>O, FeCl<sub>2</sub>.4H<sub>2</sub>O, NaOH, HCl and PEG-4000, nutrient agar from Merck. The bacteria species *Staphylococcus aureus* ATTC 25923 and *Escherichia coli* ATCC 25922 from PT Bio Farma.

### Synthesis Fe<sub>3</sub>O<sub>4</sub>-PEG 4000

The Fe<sub>3</sub>O<sub>4</sub> magnetic nanoparticles prepared by co-precipitation. Initially, 5.41 g of FeCl<sub>3</sub>.6H<sub>2</sub>O and 1.99 g of FeCl<sub>2</sub>.4H<sub>2</sub>O were added into 20 mL of distilled deionized water. Into the mixture, aqueous solution NaOH 1 M is added dropwise until pH 11 while flowing N<sub>2</sub> gas at room temperature and stirring at 200 rpm [21,22]. The magnetic nanoparticles are black precipitates, which can be separated from the solution using magnet permanent. The powder was washed using distilled water until neutral and then washed using ethanol. The product was dried under vacuum for 3 h at 60 °C. The reaction synthesis of Fe<sub>3</sub>O<sub>4</sub> by coprecipitation method is as follows:



The next step was dissolving PEG (2.50 g) in 5 mL deionized water. The solution was stirred for 30 minutes until homogeneous. Then, 0.25 g of Fe<sub>3</sub>O<sub>4</sub> was added to the suspension. The mixture was stirred under nitrogen atmosphere for 10 h at 45°C. Fe<sub>3</sub>O<sub>4</sub> coated PEG product were separated from the solution by centrifugation. Finally, the product washed with ethanol to dissolve the remaining of PEG.

The crystal structure of Fe<sub>3</sub>O<sub>4</sub>-PEG was obtained by XRD (Shimadzu XD-3H) with Cu K $\alpha$  ( $\lambda = 1.5406 \text{ \AA}$ ) radiation, magnetic properties were determined by VSM (Lake Shore 7410), in an external field (temperature in the range 10-400 K), functional group was analyzed by FTIR Shimadzu 5400 in the range 4.000-400 cm<sup>-1</sup>, morphology and element composition of Fe<sub>3</sub>O<sub>4</sub>-PEG were studied by SEM-EDX JEOL-JSM-6510 LV.

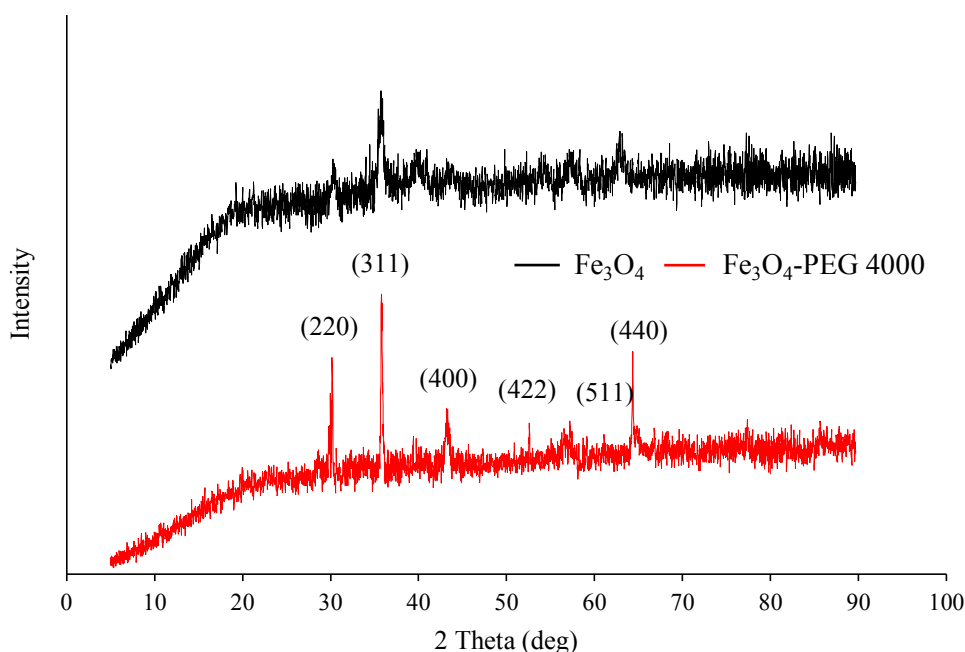
### Screening of antibacterial activities

In this study, the test of antibacterial activity was conducted using diffusion disc method [23]. The bacteria (*Staphylococcus aureus* and *Escherichia coli*) were inoculated to Petri dish with Nutrient Agar (NA) medium, then paper disc with 6 mm diameter were used to inoculated test organism.  $\text{Fe}_3\text{O}_4$ -PEG 10  $\mu\text{L}$  was instilled with different concentration (0; 12.5; 25; 50; 100 and 200  $\mu\text{g/mL}$ ). The Petri dish were wrapped by parafilm tape and then all of Petri dish were incubated at 37°C for 24 hours. The antibacterial activities were determined by measurement the zone inhibition diameter in millimeters.

## RESULT AND DISCUSSION

### Characteristic of $\text{Fe}_3\text{O}_4$ -PEG 4000

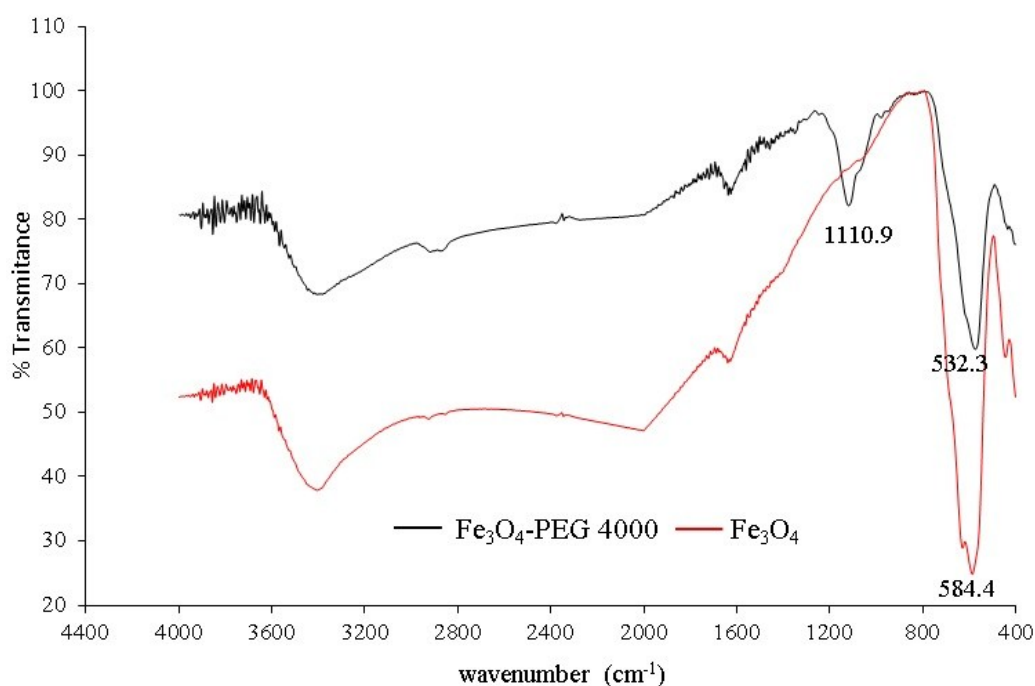
The XRD pattern of  $\text{Fe}_3\text{O}_4$  and  $\text{Fe}_3\text{O}_4$ -PEG shown in figure 1. The product has a cubic spinel structure in accordance with JCPDS 19-0629. The main peak of  $\text{Fe}_3\text{O}_4$  that appears on  $2\theta$  corresponds to the reflection planes (220), (311), (400), (422), (511) and (440). The  $\text{Fe}_3\text{O}_4$ -PEG spectra decreased in intensity due to the addition PEG which has amorphous properties. Using the Scherrer formula ( $D = 0.89\lambda/\beta \cos \theta$ ) one can estimate the average size of crystals of nanoparticles, where  $\beta$  is the full width at half maxima (FWHM). Calculation of crystal size based on the peak is highest in reflection plane of the (311) peak. It was found that the  $\text{Fe}_3\text{O}_4$ -PEG crystal size larger than  $\text{Fe}_3\text{O}_4$ . The crystallite sizes is estimated 46.2 and 35.7 nm, respectively. The similar results that  $\text{Fe}_3\text{O}_4$  nanoparticles coated using polyethyleneimine (PEI) has larger crystal size than  $\text{Fe}_3\text{O}_4$  without coating [11]. Other studies show that  $\text{CoFe}_2\text{O}_4$  nanoparticles have a smaller particle size than  $\text{CoFe}_2\text{O}_4$  that is coated using PEG [24].



**Figure 1.** XRD pattern of  $\text{Fe}_3\text{O}_4$  and  $\text{Fe}_3\text{O}_4$ -PEG 4000.

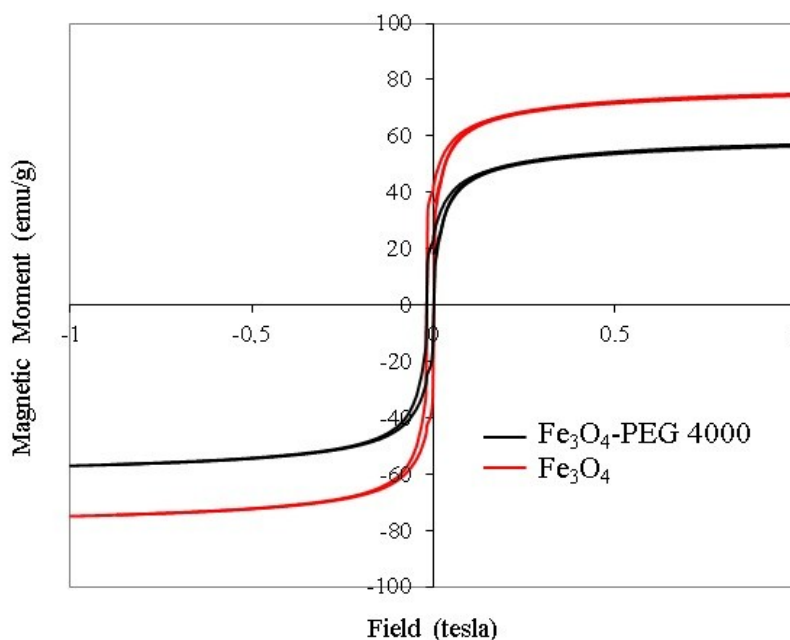
The presence of PEG on the surface of  $\text{Fe}_3\text{O}_4$  nanoparticles was evaluated by FTIR. Figure 2 displays the FTIR spectra of  $\text{Fe}_3\text{O}_4$  and  $\text{Fe}_3\text{O}_4$ -PEG 4000 at range 400-4000  $\text{cm}^{-1}$ . The peaks that appeared at the wave number 3390.6  $\text{cm}^{-1}$  on the  $\text{Fe}_3\text{O}_4$  and 3392.5  $\text{cm}^{-1}$  on

Fe<sub>3</sub>O<sub>4</sub>-PEG 4000 showed the absorption band of O-H groups from the adsorbed H<sub>2</sub>O onto materials. The peaks of Fe<sub>3</sub>O<sub>4</sub> and Fe<sub>3</sub>O<sub>4</sub>-PEG 4000 at the 1626.7 and 1627.8 cm<sup>-1</sup> indicate the bending vibrations of O-H. The characteristic peaks of PEG showed at 2862.2 and 1458.1 cm<sup>-1</sup> assigned stretching vibration and bending vibration of C-H in -CH<sub>2</sub>. The band at 1470 cm<sup>-1</sup> is C-C vibration stretching PEG. The peak that appears at 1110.9 cm<sup>-1</sup> is to the bond stretching vibrating of C-O [8]. The peak is characteristic of PEG, that does not appear on the Fe<sub>3</sub>O<sub>4</sub> spectra. The wave numbers are characteristic of Fe-O bonds shown with a strong peak at 584.4 and 532.3 cm<sup>-1</sup> on Fe<sub>3</sub>O<sub>4</sub> and Fe<sub>3</sub>O<sub>4</sub>-PEG, respectively. The shift of wave numbers of Fe-O bond on Fe<sub>3</sub>O<sub>4</sub>-PEG spectra shows the interaction between Fe<sub>3</sub>O<sub>4</sub> and PEG. Several studies have shown that the wave number of the Fe-O bond appears at 569 cm<sup>-1</sup> [20], 581 cm<sup>-1</sup> [25], and 567.12 cm<sup>-1</sup> [10].



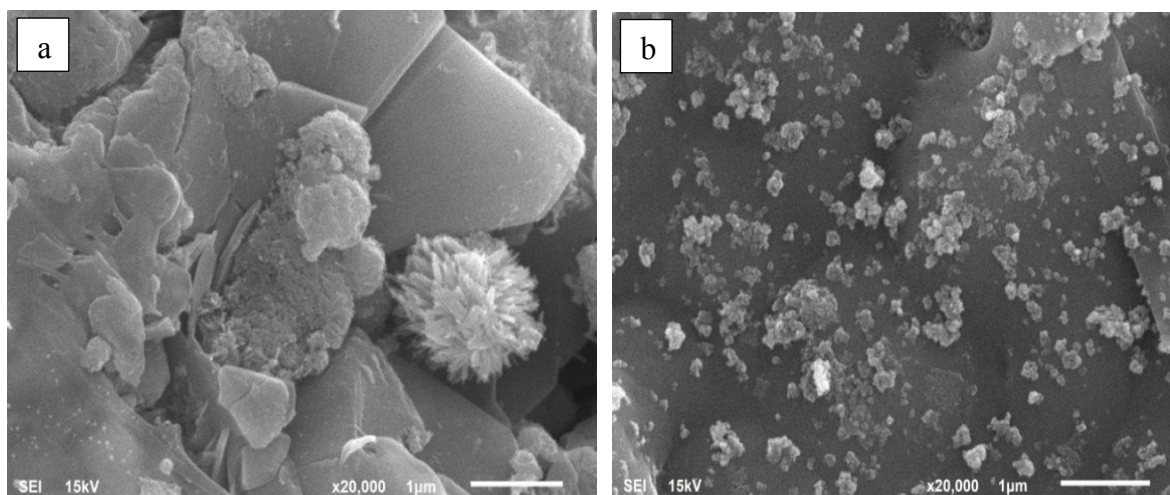
**Figure 2.** Spectra FTIR of Fe<sub>3</sub>O<sub>4</sub>-PEG 4000.

Figure 3 shows the magnetic curves of Fe<sub>3</sub>O<sub>4</sub> and Fe<sub>3</sub>O<sub>4</sub>-PEG. It reveals that Fe<sub>3</sub>O<sub>4</sub> has high saturation magnetization than Fe<sub>3</sub>O<sub>4</sub>-PEG. The addition of organic polymers (PEG) causes a small reduction in magnetic properties. Fe<sub>3</sub>O<sub>4</sub>-PEG is classified as superparamagnetic which in this research shows saturation magnetization of 56.43 emu/g while Fe<sub>3</sub>O<sub>4</sub> is 74.33 emu/g. The changes in magnetic properties due to the effect of surface modification of Fe<sub>3</sub>O<sub>4</sub> by large polymer molecules. The greater the concentration of PEG is added, the lesser of the saturation magnetization where the polymer coat the nanoparticles so that giving a protection effect from the magnetic field [24]. The saturation magnetization value is similar to the other reference [20,25]. Their study reported Fe<sub>3</sub>O<sub>4</sub> modified with sodium citrate and oleic acid with various concentrations of Fe<sub>3</sub>O<sub>4</sub> showed magnetization saturation of 50.61 – 61.36 emu/g [25].



**Figure 3.** The saturation magnetization of  $\text{Fe}_3\text{O}_4$  and  $\text{Fe}_3\text{O}_4$ -PEG 4000.

The morphology of  $\text{Fe}_3\text{O}_4$  and  $\text{Fe}_3\text{O}_4$ -PEG 4000 and its constituent elements were analyzed using SEM-EDX. SEM image of  $\text{Fe}_3\text{O}_4$  and  $\text{Fe}_3\text{O}_4$ -PEG 4000 are displayed in figure 4. The image shows a clear difference between  $\text{Fe}_3\text{O}_4$  before and after modification with PEG. The morphology of  $\text{Fe}_3\text{O}_4$  appears to be agglomerated while modified with PEG appears to be dispersed on PEG surface.



**Figure 4.** SEM image of (a)  $\text{Fe}_3\text{O}_4$  and (b)  $\text{Fe}_3\text{O}_4$ -PEG 4000

Table 1 shows the constituent elements of  $\text{Fe}_3\text{O}_4$  and  $\text{Fe}_3\text{O}_4$ -PEG 4000. It can be seen that the addition of carbon elements in  $\text{Fe}_3\text{O}_4$ -PEG 4000 indicates that modification of  $\text{Fe}_3\text{O}_4$ -PEG is successful. The main elements of  $\text{Fe}_3\text{O}_4$  are Fe and O while modified of  $\text{Fe}_3\text{O}_4$  with PEG affects as the percentage of C element increases.



**Table 1.** The data of elements Fe<sub>3</sub>O<sub>4</sub> and Fe<sub>3</sub>O<sub>4</sub>-PEG 4000

Materials	Mass (%)		
	Fe	O	C
Fe <sub>3</sub> O <sub>4</sub>	43.36	56.98	-
Fe <sub>3</sub> O <sub>4</sub> -PEG 4000	26.80	38.93	34.27

### Antibacterial activity

Antibacterial activities in this study show in figure 5 and table 2. In the figure, we can see that zone of inhibition of Fe<sub>3</sub>O<sub>4</sub>-PEG 4000 to *Staphylococcus aureus* and *Escherichia coli*. The different concentrations of Fe<sub>3</sub>O<sub>4</sub>-PEG 4000 give different diameter of inhibition zone. The size of the inhibitory zone depends on the type of bacteria, the size, and concentration of the nanoparticles [26]. The antibacterial activity of Fe<sub>3</sub>O<sub>4</sub> can be explained that Fe<sub>3</sub>O<sub>4</sub> is positively charged while the bacterium is negatively charged, so there is an interesting attraction between Fe<sub>3</sub>O<sub>4</sub> and bacteria. Bacteria is oxidized and dies [4]. In this study, it appears that gram-positive bacteria has a smaller diameter of inhibition zone than that in gram-negative bacteria. Another study, also suggest that the gram-negative bacteria are more sensitive compare to gram-positive bacteria [4].

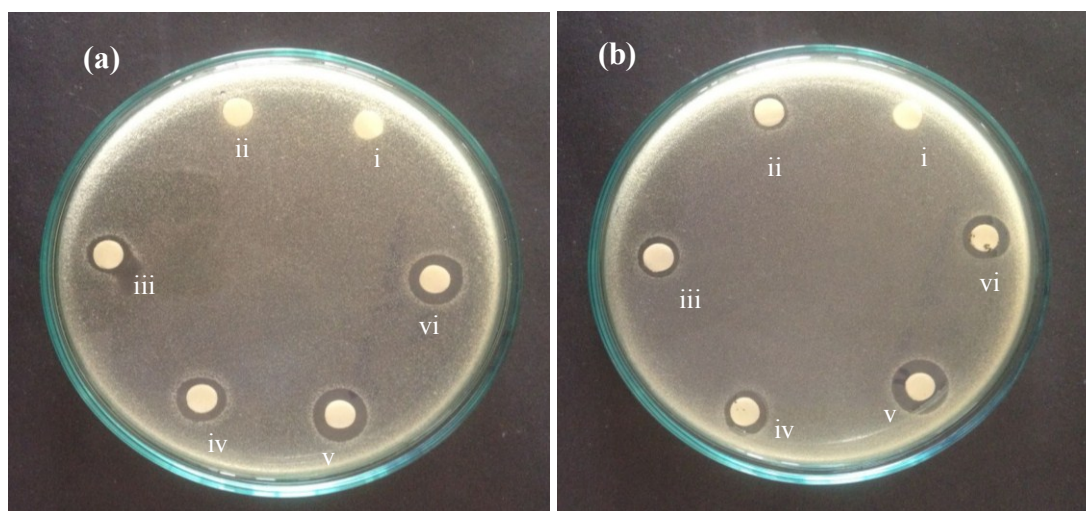


**Figure 5.** Antibacterial activity of Fe<sub>3</sub>O<sub>4</sub>-PEG 4000 with concentration (i)0 (ii)12.5 (iii)25 (iv)50 (v)100 and (vi)200 µg/mL to (a) *Staphylococcus aureus* and (b) *Escherichia coli* (give information number in image; the number refer to concentration sample in ppm or other)

The same result was reported previously, that gram-negative have higher susceptibility than gram-positive bacteria. The killing rate of *Escherichia coli* is higher than that in *Staphylococcus aureus* [27]. The differences in susceptibility are caused by differences in cell wall structures, cell physiology and metabolism [15,28]. PEG was also reported to have antibacterial activity. The hydrophilic properties of PEG inhibit bacterial growth. Water is very important for bacteria for growth and multiplication [29]. The MIC (Minimum Inhibitory Concentration) for *Staphylococcus aureus* is 12.5 µg/mL with an average of inhibitory diameter 6.6 mm, and this result is smaller than that in *Escherichia coli* with an average of inhibitory diameter 6.3 mm at concentration 25 µg/mL.

**Table 2.** The diameter of inhibition zone for Fe<sub>3</sub>O<sub>4</sub>-PEG 4000

Concentration (µg/mL)	Average inhibitory diameter (mm)	
	<i>Staphylococcus aureus</i>	<i>Escherichia coli</i>
200	11.0	10.2
100	11.1	11.3
50	7.3	8.4
25	6.3	7.2
12.5	0	6.6
0	0	0

## CONCLUSION

Fe<sub>3</sub>O<sub>4</sub> nanoparticles modified with PEG could be used as an antibacterial material. The Fe<sub>3</sub>O<sub>4</sub>-PEG showed antibacterial properties on gram-positive and gram-negative bacterial strains. The antibacterial effect of Fe<sub>3</sub>O<sub>4</sub>-PEG on *Escherichia coli* is stronger than *Staphylococcus aureus*. The MIC value of Fe<sub>3</sub>O<sub>4</sub>-PEG for *Escherichia coli* is 12.5 µg/mL whilst for *Staphylococcus aureus* is 25 µg/mL. These results suggest that the Fe<sub>3</sub>O<sub>4</sub>-PEG has a potential application, and further research has to be undertaken for toxicity evaluation in the animal model or human.

## ACKNOWLEDGMENT

The financial support of the research by Sriwijaya University for Unggulan Kompetitif Universitas Sriwijaya Research Grant No. 988/UN9.3.1/PP/2017.

## REFERENCES

- [1] Sharma, Y.C., and Srivastava, V., *J. Chem. Eng. Data*, **2011**, 56, 819–825.
- [2] Shahriari, T., Bidhendi, G.B., Mehrdadi, N., *Int. J. Environ. Sci. Technol.*, **2014**, 11, 349–356.
- [3] Sam, S., and Nesaraj, A.S., *Int. J. Appl. Sci. Eng.*, **2011**, 9(4), 223–239.
- [4] Prabhu, Y. T., and Rao, K. V., *Int. Nano Lett.*, **2015**, 5, 85–92.
- [5] Vignesh, R. H., Sankar, K.V., Amaresh, S., Lee, Y.S., Selvan, R.K., *Sensor Actuat B-Chem.*, **2015**, 220, 50–58.
- [6] Iwasaki, T., Mizutani, N., Watano, S., Yanagida, T., Kawai, T., *J. Exp. Nano Sci.*, **2010**, 5(3), 251–262.
- [7] Chen, F., Xie, S., Zhang, J., Liu, R., *Mater. Lett.*, **2013**, 112, 177–179.
- [8] Lei, W., Liu, Y., Si, X., Xu, J., Du, W., Yang, J., Zhou, T., Lin, J., *Phys. Lett. A*, **2016**, 381(16), 1–5.
- [9] Zhou, Z. H., Wang, J., Liu, X., Chan, H. S. O., *J. Mater. Chem.*, **2001**, 11, 1709–1711.
- [10] Es'haghzade, Z., Pajootan, E., Bahrami, H., Arami, M., *J. Taiwan Inst. Chem. Eng.*, **2016**, 9(54), 1–15.
- [11] Karimzadeh, I., Aghazadeh, M., Doroudi, T., Ganjali, M. R., Kolivand, P. H., *Adv. in Phys. Chem.*, **2017**, 1–8.
- [12] Shanmugavel, T., Raj, S. G., Kumar, G. R., Rajarajan, G., *Phys. Procedia*, **2014**, 54, 159–163.
- [13] Sharafi, A., and Seyedsadjadi, M., *Int. J. Bio-Inorg. Hybd. Nanomat.*, **2013**, 2(3), 437–441.
- [14] Behera, S.S., Patra, J.K., Pramanik, K., Panda, N., Thatoi, H., *World J. Nano Sci. Eng.*, **2012**, 2, 196–200.

- [15] Shahzeidi, Z. S., and Amiri, Gh., *Int. J. Bio-Inorg. Hybd. Nanomat.*, **2015**, 4(3), 135–140.
- [16] Topkaya, R., Kurtan, U., Baykal, A., Sozeri, K., Toprak, M. S., *J. Inorg Organomet Polym.*, **2013**, 23, 592–598.
- [17] Junejo, Y., Baykal, A., Sozeri, H., *Cent. Eur. J. Chem.*, **2013**, 11(9), 1527–1532.
- [18] Tamhakar, P.M., Kulkarni, A.M., Watawe, S.C., *Mater. Sci. App.*, **2011**, 2, 1317–1321.
- [19] Zheng, X. F., and Lian, Q., *J. Disper. Sci. Technol.*, **2015**, 36, 245–251.
- [20] Mukhopadhyay, A., Joshi, N., Chattopadhyay, K., De, G., *ACS Appl. Mater. Interfaces.*, **2012**, 4, 142–149.
- [21] Hariani, P. L., Faizal, M., Ridwan, Marsi, Setiabudidaya, D., *Int. J. Env. Sci. Dev.*, **2013**, 4(3), 336–340.
- [22] Zhu, H. Y., Fu, Y. Q., Jiang, R., Jiang, J. H., Xiao, L., Zeng, G. M., Zhao, S.L., Wang, L., *Chem. Eng. J.*, **2011**, 173, 494 – 502.
- [23] Paredes, D., Ortiz, C., Torres, *Int. J. Nanomed.*, **2014**, 9, 1717–1729.
- [24] Sulanjari., Santi, W. N., Artanti, A. A., Suharyadi, E., Kato, E., Iwata, S., *JFI*, **2014**, 54, XVIII, 103–107.
- [25] Wei, Y., Han, B., Hu, X., Lin, Y., Wang, X., Deng, X., *Procedia Engineering*, **2012**, 27, 632 – 637.
- [26] Reddy, D. H. K., and Yun, Y. S., *Coord. Chem. Rev.*, **2016**, 315, 90 – 111.
- [27] Atmaca, S., Gul, K., Cicek., R., *Tr. J. of Medical Science*, **1998**, 28, 595 – 597.
- [28] Sanpo, N., Wen, C., Berndt, C., Wang, J., Antibacterial Properties of Spinel Ferrite Nanoparticles in Microbacterial pathogens and strategies for combating them: science, technology and education, **2013**, Formatex Research Center, Spain.
- [29] Nalawade, T.M., Bhat, K., Sogi, S. H. P., *J. Int. Soc. Prev. Comm. Dent.*, **2015**, 5(2), 114–119.